

Published in final edited form as:

*Sci Total Environ.* 2011 July 1; 409(15): 2942–2950. doi:10.1016/j.scitotenv.2011.04.021.

## Atmospheric concentrations and air–soil gas exchange of polycyclic aromatic hydrocarbons (PAHs) in remote, rural village and urban areas of Beijing–Tianjin region, North China

Wentao Wang<sup>a,b,c</sup>, Staci Simonich<sup>c</sup>, Basant Giri<sup>c,d</sup>, Ying Chang<sup>b</sup>, Yuguang Zhang<sup>e</sup>, Yuling Jia<sup>c</sup>, Shu Tao<sup>a,\*</sup>, Rong Wang<sup>a</sup>, Bin Wang<sup>a</sup>, Wei Li<sup>a</sup>, Jun Cao<sup>a</sup>, and Xiaoxia Lu<sup>a</sup>

<sup>a</sup>Laboratory for Earth Surface Processes, College of Urban and Environmental Sciences, Peking University, Beijing 100871, China

<sup>b</sup>The Administrative Center for China's Agenda 21 (ACCA21), Ministry of Science and Technology, Beijing, 100038, China

<sup>c</sup>Department of Environmental and Molecular Toxicology and Department of Chemistry, Oregon State University, Corvallis, Oregon, 97331, USA

<sup>d</sup>Department of Chemistry, University of Wyoming, Laramie, Wyoming, 83072, USA

<sup>e</sup>Institute of Forestry Ecology, Environment and Protection, and the Key Laboratory of Forest Ecology and Environment of State Forestry Administration, the Chinese Academy of Forestry, Beijing 100091, China

### Abstract

Forty passive air samplers were deployed to study the occurrence of gas and particulate phase PAHs in remote, rural village and urban areas of Beijing–Tianjin region, North China for four seasons (spring, summer, fall and winter) from 2007 to 2008. The influence of emissions on the spatial distribution pattern of air PAH concentrations was addressed. In addition, the air–soil gas exchange of PAHs was studied using fugacity calculations. The median gaseous and particulate phase PAH concentrations were 222 ng/m<sup>3</sup> and 114 ng/m<sup>3</sup>, respectively, with a median total PAH concentration of 349 ng/m<sup>3</sup>. Higher PAH concentrations were measured in winter than in other seasons. Air PAH concentrations measured at the rural villages and urban sites in the northern mountain region were significantly lower than those measured at sites in the southern plain during all seasons. However, there was no significant difference in PAH concentrations between the rural villages and urban sites in the northern and southern areas. This urban–rural PAH distribution pattern was related to the location of PAH emission sources and the population distribution. The location of PAH emission sources explained 56%–77% of the spatial variation in ambient air PAH concentrations. The annual median air–soil gas exchange flux of PAHs was 42.2 ng/m<sup>2</sup>/day from soil to air. Among the 15 PAHs measured, acenaphthylene (ACY) and acenaphthene (ACE) contributed to more than half of the total exchange flux. Furthermore, the air–soil gas exchange fluxes of PAHs at the urban sites were higher than those at the remote and rural sites. In summer, more gaseous PAHs volatilized from soil to air because of higher temperatures and increased rainfall. However, in winter, more gaseous PAHs deposited from air to soil due to higher PAH emissions and lower temperatures. The soil TOC concentration had no significant influence on the air–soil gas exchange of PAHs.

## Keywords

Atmospheric PAHs; Passive air sampling; Air; soil exchange; Beijing; Tianjin

---

## 1. Introduction

Polycyclic aromatic hydrocarbons (PAHs) are ubiquitous environmental contaminants that are formed mainly during incomplete combustion of fossil fuels and biomass. Chinese PAH emissions contributed to over 20% of the total global PAH emissions in 2004 (Zhang and Tao, 2008). As a result, PAH emissions in excess of 116,000 tons/year have resulted in the contamination of various environmental media in China, especially ambient air (Zhang et al., 2007). In addition, it was reported by Zhang et al. (2009) that 1.6% of the lung cancer morbidity in China was due to inhalation exposure to ambient air PAHs.

Air–soil exchange is one of the most important processes governing the fate of persistent organic pollutants (POPs), including PAHs, in the environment (Cousins et al., 1999) and understanding their air–soil exchange is important for evaluating the risk associated with environmental contamination and human exposure. Previous studies have focused on the air–soil exchange of organochlorine pesticides (OCPs) (Harner et al., 2001; Meijer et al., 2003a, b; Bidleman and Leone, 2004; Kurt-Karakus et al., 2006; R ž i ková et al., 2008; Tao et al., 2008; Bozlaker et al., 2009; Kobližková et al., 2009; Wong et al., 2010), polychlorinated biphenyls (PCBs) (Harner et al., 1995; Cousins and Jones, 1998; Backea et al., 2004; Bozlaker et al., 2008a; R ž i ková et al., 2008; Kobližková et al., 2009; Li et al., 2010), polychlorinated dibenzo-p-dioxins (PCDDs) (Cousins et al., 1998), and polybrominated diphenyl ethers (PBDEs) (Cetin and Odabasi, 2007). However, there is a limited number of studies on the air–soil exchange of PAHs (Bozlaker et al., 2008b; Wang et al., 2008a). Multimedia fugacity and atmospheric dispersion models predict that air–soil exchange of PAHs may be one of the most significant processes for removing PAHs from the atmosphere, as well as the most important process for contaminating soils with PAHs (Lang et al., 2007).

Beijing and Tianjin are two of the largest cities in northern China and the rapid population growth, industrialization and urbanization of this area during the last decade have resulted in high PAH emissions (Zhang et al., 2007) and high atmospheric concentrations (Zhou et al., 2005; Okuda et al., 2006; Wu et al., 2006, 2007; Wang et al., 2008b; Zhang et al., 2009). Recently, Liu et al. (2007, 2008) reported that atmospheric PAH concentrations in rural Chinese villages are similar to, or even higher than, those in urban areas due to the extensive use of biomass and coal as fuels for cooking and heating. Given this, it is important to further investigate this finding and assess the air–soil exchange of PAHs in rural villages and urban areas in the Beijing–Tianjin area.

The objectives of this study were to (1) investigate the seasonal variation and spatial distribution of the atmospheric PAH concentrations in this region, (2) determine the magnitude and direction of air–soil gas exchange of PAHs in remote, rural village and urban areas, (3) investigate the seasonal variation and spatial distribution of the air–soil gas exchange fluxes of PAHs, and (4) assess the influence of PAH emission density, total organic carbon (TOC) concentration in soil, and temperature, on the air–soil gas exchange of PAHs.

## 2. Materials and methods

### 2.1. Sampling

Passive air samplers with PUF (polyurethane foam) disks and glass fiber filter (GFF) were used to collect PAHs in the gas and particulate phase, respectively. The sampler has been tested in field conditions at different meteorological conditions with satisfaction and detailed calibration and uptake rates of this sampler were described previously (Tao et al., 2009). It is important to note that this passive air sampler samples the particle-bound PAHs less efficiently than gas-phase PAHs. Therefore, higher uncertainties are associated with the measured particle-phase PAH concentrations in this study. Passive air sampling data were collected at 40 remote, rural village and urban sites between 2007 and 2008 covering four seasons, and the sampling period in winter included the residential heating time. Two identical samplers were deployed at each site on rooftops or in open areas at each site at 1.5 to 20 m high off the ground in order to avoid airflow obstruction. The passive air samplers were mounted at different heights because of logistical constraints. PAH concentrations may change over height, the effect of sampling height on the result could be a constrain of the method and the results should be interpolated with care.

Soil samples were collected from the same sampling sites in September 2007 (Wang et al., 2010). Briefly, surface soils (0–5 cm in depth) were collected using a stainless steel soil corer after the upper organic vegetative material was removed. Five soil samples were collected over a 100 m<sup>2</sup> area, pooled and homogenized to obtain a composite soil sample. Detailed sampling information, including the sampling height, longitude, latitude and sampling periods are given in Table S1.

The study area covers Beijing, Tianjin and part of the Hebei province (50,000 km<sup>2</sup>, with 70 million inhabitants) (Fig. S1) and all of the sampling sites were located far from industrial areas and roadsides. The northern and southern rural villages and northern and southern urban areas were divided based on a boundary line between the mountain area and the plain area of the Beijing–Tianjin region (Fig. S1). This separation between the northern and southern sites is demonstrated by a scatter plot of gross domestic product (GDP) and population density for northern rural villages, southern rural villages, northern urban areas and southern urban areas (Fig. S2).

After sampling, all PUF disks were stored at –18 °C. The GFFs were equilibrated in a desiccator (25 °C) for 24 h and weighed before and after the sampling, in accordance with USEPA Method 5 of 40 CFR Part 60 (<http://www.epa.gov/ttn/emc/methods/method5.html>). It is likely that the particles will adjust to a new equilibrium with the air inside the desiccators, which brings uncertainties to the following sample extraction and analysis. Before sampling, the PUF disks were pre-cleaned in a Soxhlet extractor with dichloromethane for 24 h and the GFFs were prebaked in a furnace at 450 °C for 4 h.

### 2.2. Extraction and analysis

PUF disks and GFFs were Soxhlet extracted with 100 mL dichloromethane for 12 h (Liu et al., 2007; Tao et al., 2009), and the extracts were concentrated by rotary evaporation to about 1.0 mL, solvent exchanged to *n*-hexane, and purified on an alumina silica packed column (10 cm, 3% deactivated silica gel, 6 cm, 3% deactivated alumina, and 1 cm anhydrous sodium sulfate). The silica gel, alumina and anhydrous sodium sulfate were baked at 450 °C for 4 h prior to use. The column was eluted with 50 mL of dichloromethane/hexane (2:3) at a rate of 2 mL/min to yield the PAHs fraction. The eluant was concentrated on the rotary evaporator at below 38 °C to approximate 1 mL.

Fifteen PAHs, including acenaphthene (ACE), acenaphthylene (ACY), fluorene (FLO), phenanthrene (PHE), anthracene (ANT), fluoranthene (FLA), pyrene (PYP), benz(a)anthracene (BaA), chrysene (CHR), benzo (b)-fluoranthene (BbF), benzo(k)fluoranthene (BkF), benzo(a)pyrene (BaP), dibenzo(a,h)anthracene (DahA), indeno(1,2,3-cd)pyrene (IcdP), and benzo(ghi)perylene (BghiP), were analyzed on a gas chromatograph (Agilent 6890) coupled to a mass selective detector (MSD, Agilent 5973). Twenty percent of the samples were spiked with deuterated PAHs (NAP- $d_8$ , ANE- $d_{10}$ , ACE- $d_{10}$ , ANT- $d_{10}$ , CHR- $d_{12}$  and Perelyne- $d_{12}$ ) before extraction to monitor the loss of PAHs during extraction and cleanup procedures. 2-fluoro-1,1'-biphenyl and *p*-terphenyl- $d_{14}$  (2.0  $\mu\text{g/mL}$ , J&K Chem, USA) were spiked onto the samples and used as internal standards for quantification of the 15 PAHs in each sample. Details of the analysis and quantification methods have been described previously (Liu et al., 2007). All solvents were of analytical grade and redistilled. All glassware was cleaned using an ultrasonic cleaner (Kunshan KQ-500B, China) and baked at 400 °C for 6 h.

### 2.3. Quality control and quality assurance

Thirty-two field blanks, including a PUF and GFF, were analyzed. The instrumental detection limits and the concentration range of PAHs in the field blank samples are shown in Table S2. The PAH concentrations in blank samples were at least one order of magnitude lower than the actual samples. The reported sample PAH concentrations were blank subtracted using the mean of all blanks. Method recoveries were determined by spiking the standard mixture of 15 PAHs onto the PUF disks and GFFs and performing the entire analytical methods. The recoveries were 79–114% for the PUF disks and 72–102% for the GFFs. The recoveries for the deuterated PAHs were 79–96% for the PUF disks and 73–91% for the GFFs. The average coefficients of variation for PAH concentrations measured in duplicate samples were 3–18% for the PUF disks and 4–28% for the GFFs. The same quality control steps are also used in other studies (Liu et al., 2007, 2008; Tao et al., 2009; Wang et al., 2010).

## 3. Results and discussion

### 3.1. PAHs concentration in air

The annual median air PAH concentration for the entire study region was 222  $\text{ng/m}^3$  for the gaseous PAHs, 114  $\text{ng/m}^3$  for the particulate PAHs, and 349  $\text{ng/m}^3$  for the total 15PAHs (sum of gaseous and particulate-phase) (Tables S4, S5, and S6). Compared with other regions in the world (Table S3), the Beijing–Tianjin region is more severely contaminated with PAHs. However, although the passive air samplers used in this study were well characterized and calibrated, these results may not be directly comparable to previous studies using a high volume sampling method (Tao et al., 2009).

In general, the lower molecular weight PAHs (ACE, ACY, FLO, PHE, and ANT) were primarily measured in the gas-phase (Table S4), and the higher molecular weight PAHs (PYP, BaA, CHR, BbF, BkF, BaP, DahA, IcdP, and BghiP) were primarily measured in the particulate phase (Table S5).

### 3.2. Seasonal variation and spatial distribution of PAHs in air

The median concentrations of all 15 PAHs in the gaseous, particulate and sum of gaseous and particulate phases in this study were 169  $\text{ng/m}^3$ , 72.5  $\text{ng/m}^3$  and 252  $\text{ng/m}^3$  in spring, 120  $\text{ng/m}^3$ , 28.8  $\text{ng/m}^3$  and 145  $\text{ng/m}^3$  in summer, 222  $\text{ng/m}^3$ , 154  $\text{ng/m}^3$  and 377  $\text{ng/m}^3$  in fall, and 346  $\text{ng/m}^3$ , 146  $\text{ng/m}^3$  and 521  $\text{ng/m}^3$  in winter. (Tables S4, S5, S6). Total PAH concentrations in summer were significantly lower compared to the other three seasons ( $p < 0.01$ ). Similarly, total PAH concentrations in spring were significantly lower compared to

fall and winter ( $p < 0.01$ ). However, there was no significant difference between total PAH concentrations in fall and winter ( $p > 0.05$ ). In the Beijing–Tianjin region, the main PAH emission sources are the domestic burning of coal, straw and firewood, which account for 75% of the total PAH emission (Zhang et al., 2007). The increase in PAH concentrations during colder weather is likely due to residential heating with biomass and domestic coal combustion (Liu et al., 2007). Moreover, atmospheric photochemical degradation of PAHs and precipitation in this region are more significant during summer, which may decrease PAH concentrations. A significant difference in PAH concentrations between winter and summer was also reported in other studies (Bozlaker et al., 2008b; Zhou et al., 2005; Wang et al., 2008b; Wu et al., 2007; Liu et al., 2008). The individual PAH concentrations and profile distribution in spring, summer, fall and winter are shown in Fig. S3. Higher PHE, FLO and FLA concentrations were measured in the winter, while higher DahA and IcdP concentrations were measured in the summer, likely because of different combustion source types.

Gaseous and particulate phase PAH concentrations tend to follow similar spatial distribution patterns on regional scales (Sun et al., 2006; Liu et al., 2008). This pattern was also observed in this study and gaseous phase PAH concentrations were positively correlated with particulate phase PAH concentrations in all seasons ( $n = 40$ ,  $p < 0.001$ ). Therefore, the total PAH concentration was used for the spatial distribution analysis.

The geographic distribution of total PAH concentrations in all four seasons is shown in Fig. S4. The most contaminated areas were the urban areas of Beijing and Tianjin, east and southwest areas of Hebei, and a number of large cities, including Tangshan, Baoding, Cangzhou and Langfang. The areas with the lowest PAH concentrations were mountain areas in northwest Hebei (Zhangjiakou) and north of Beijing (Huairou) that have a relatively low population density and are less developed. The spatial distribution of PAH emission sources is likely to influence the spatial distribution pattern of atmospheric PAH concentrations. For example, the annual average total PAH concentrations in air from Xiaolongmen (background site), Shijing (rural village site), and Tangshan (urban site) were 39.4, 355, and 1010  $\text{ng}/\text{m}^3$ , respectively. These concentrations correlate with the PAH emission density of 0.84  $\text{kg}/\text{m}^2/\text{year}$  in Xiaolongmen, 32.3  $\text{kg}/\text{m}^2/\text{year}$  in Shijing, and 135  $\text{kg}/\text{m}^2/\text{year}$  in Tangshan. Klánová et al. (2006) measured atmospheric PAH concentrations in several cities in the Czech Republic and found that the ambient air PAH concentrations were significantly affected by local emissions. Gioia et al. (2007) also found that the ambient air PAH concentrations were more closely related to emissions from the adjacent source country rather than remote ones. In addition, Liu et al. (2008) obtained a good correlation between high-resolution PAH emission data and atmospheric PAH concentrations in the North China Plain. In the current study, a linear correlation between log transformed air PAH concentration and log-transformed PAH emission density was measured (Fig. 1), using high-resolution PAH emission rates in all four seasons from Zhang and Tao (2009). Approximately 67, 56, 70, and 77% of the spatial variation in air PAH concentrations can be explained by PAH emission sources in spring, summer, fall, and winter, respectively.

The annual average of air total PAH concentrations in the remote (2 sites), northern rural village (13 sites), south rural village (11 sites), north urban (4 sites) and south urban (10 sites) areas were  $50.5 \pm 15.7$ ,  $225 \pm 81.0$ ,  $418 \pm 88.0$ ,  $310 \pm 69.5$ , and  $567 \pm 203$   $\text{ng}/\text{m}^3$ , respectively. The PAH concentrations measured at the rural villages and urban sites in the northern mountain region were significantly lower than those measured at the sites in the southern plain during all seasons ( $p < 0.05$ ). However, there was no significant difference in PAH concentrations between the rural villages and urban sites in northern/southern areas ( $p > 0.05$ ). Similar trends were found for each season and for individual PAHs (Fig. 2).



Hafner et al. (2005) reported that there was a significant correlation between air PAH concentrations and population density. A large population density and increased human activities often result in higher energy consumption rates and higher emission rates of incomplete combustion products, including PAHs. This is particularly true for areas with similar energy consumption patterns. In this study, 68–79% of total spatial variation in remote, rural village and urban area PAH concentrations can be explained by population density in all four seasons (Fig. S5). In addition, there was good separation between remote, northern rural village and urban areas, and southern rural village and urban areas, because of different energy consumption patterns. In rural villages, the dominant PAH emission sources are indoor biomass burning and domestic coal combustion for cooking and heating (Liu et al., 2008). These less energy-efficient practices in villages result in higher PAH emissions compared to coal combustion and vehicle emissions in urban areas. In addition, in cities, centralized heating system with industrial boilers and the use of natural gas in homes decrease the need for biomass or domestic coal stoves. In this study, the southern plain area is more developed than the northern region (Figs. S1, S2, S5), which results in more energy consumption and more PAH emissions in the south rather than in the north (Fig. 1). In addition, 60–74% of the total spatial variation in air PAH concentration is explained by local GDP (gross domestic product) (Fig. S5). It has been demonstrated that PAH emission density, population density and GDP are positively correlated with each other (Zhang et al., 2007) and are important for explaining the spatial variation of PAH concentrations for different seasons.

### 3.3. Air–soil gas exchange of PAHs

The fugacity fraction ( $f_f$ ) is calculated as the fugacity in soil divided by the sum of fugacities in soil and air and serves as an indication of the net direction of air–soil gas exchange of PAHs (Harner et al., 2001).

$$f_f = f_s / (f_s + f_a) \quad (1)$$

Detailed fugacity calculations for air and soil can be found in Mackay (1979) and are also provided in the supplementary material. In this study, the soil PAH fugacity ( $f_s$ ) was calculated from the soil PAH concentrations reported in Wang et al. (2010), and the atmospheric PAH fugacity ( $f_a$ ) was calculated from the atmospheric gas phase PAH concentrations in this study in different seasons. A fugacity fraction of ~0.5 indicates equilibrium, > 0.5 indicates net volatilization from the soil into air, and < 0.5 indicates net deposition from air to soil. However, due to uncertainties and the propagation of errors in the calculation, fugacity fractions between 0.3 and 0.7 were not considered to differ significantly from equilibrium,  $f_f > 0.7$  indicated that the soil was a source with net volatilization from soil to air, and  $f_f < 0.3$  indicated that the soil was a sink with net deposition from air to soil (Harner et al., 2001; Meijer et al., 2003a, b).

The  $f_f$  values for individual PAH in all four seasons are shown in Fig. 3 and in the box-and-whisker plot is shown in Fig. S6. In general, the  $f_f$  values increased with decreased molecular weight of the individual PAHs. In addition, there were significant differences between the  $f_f$  values in summer and winter for all individual PAHs ( $p < 0.01$ ), with all of the  $f_f$  values in summer being greater than the corresponding winter values. This indicated that there was a higher tendency for PAHs to volatilize from soil to air during the summer. In summer, the  $f_f$  values for lower molecular weight (LMW) PAHs (ACE, ACY, FLO and PHE) were greater than 0.7, indicating that soil acted as a secondary source to the atmosphere for the PAHs. The  $f_f$  values for ANT, FLA, PYR, BaA, CHR, BbF, BkF and IcdP indicated that the soil and air were close to equilibrium for these compounds and the  $f_f$  values for BaP, DahA and BghiP, indicated that soil was a sink for these higher molecular

weight (HMW) PAHs from the atmosphere (Fig. 3). In winter, soil was a sink and there was net deposition for all PAHs, except for ACE and ACY. Similar  $f_f$  values were calculated for spring and fall. Due to their higher volatility and lower retention in soil, LMW PAHs are more mobile and subject to soil–air transfer (Hippelein and McLachlan, 1998; Cousins et al., 1999). Once deposited, the HMW PAHs tend to accumulate in soil for longer periods. Cousins and Jones (1998) and Wang et al. (2008a) reported that soil was a source of some LMW PAHs to the atmosphere and a long-term sink for HMW PAHs. These results were also consistent with a previous study by Bozlaker et al. (2008b), in which the air–soil partitioning of the medium volatility PAHs was found to be more sensitive to the seasonal air concentrations and temperature variations than the lower and higher volatility PAHs, as indicated by their shift from volatilization to deposition from summer to winter.

The  $f_f$  values in remote, north rural village, south rural village, north urban and south urban areas are presented in Fig. S7. In general, larger  $f_f$  values were calculated for urban villages relative to rural villages and remote areas in all seasons, indicating that PAHs had a higher tendency to volatilize from soil to air in urban areas rather than in rural village and remote areas. This finding is consistent with a previous study in Dalian, China (Wang et al., 2008a). In addition, a one-way ANOVA test showed that there were no significant differences for ACE, ACY, FLO and PHE in  $f_f$  values in the five different study areas ( $p > 0.05$ ). However, in summer,  $f_f$  values of individual PAHs (excluding ACE, ACY, FLO and PHE) in remote areas were significantly lower compared to other regions, and were significantly lower in northern rural villages compared to southern urban areas. This indicated that there were higher PAH evaporation rates from soil in southern urban areas than in remote and northern village areas.

### 3.4. Air–soil gas exchange flux of PAHs

The net air–soil gas exchange flux is driven by the fugacity difference between air and surface soil (Mackay and Paterson, 1991), and the detailed calculation method for air–soil exchange flux of gaseous PAH has been reported by Mackay (1991) and Backea et al. (2004), and is presented in the supplementary material.

The results of air–soil gas exchange flux of PAHs are shown in Table S7. The negative flux value suggests that the air–soil gas exchange direction of PAHs from soil to air, and the positive flux value suggests that the air–soil gas exchange direction of PAHs from air to soil. The median of air–soil gas exchange fluxes of 15 PAHs were  $-56.4$ ,  $-385$ ,  $-4.03$ , and  $233$   $\text{ng/m}^2/\text{day}$  in spring, summer, fall, and winter, respectively. The annual median flux of PAHs was  $-42.2$   $\text{ng/m}^2/\text{day}$ , equivalent to  $4.1$   $\text{ng/m}^2/\text{year}$  evaporation as  $\text{BaP}_{\text{eq}}$  (benzo(a)pyrene equivalent concentration) from soil to air, based on toxic equivalent factors from Nisbet and Lagoy (1992). This is also equivalent to  $\sim 2.1$  kg PAHs evaporated as  $\text{BaP}_{\text{eq}}$  from soil in this region ( $50,000$   $\text{km}^2$ ) every year. The highest deposition flux from air to soil and evaporation flux of total gaseous PAHs occurred in winter in Tangshan ( $741$   $\text{ng/m}^2/\text{day}$ ) and in summer in Baodi ( $2150$   $\text{ng/m}^2/\text{day}$ ). There was more gaseous PAH evaporation from soil to air in summer than in other seasons, and in winter more gaseous PAHs deposited from air to soil. The low molecular weight PAHs, including ACY, FLO, ACE, ANT, and PHE, are the most important PAHs for air–soil gas exchange. The high molecular weight PAHs are less important during air–soil gas exchange due to very low concentrations in the atmosphere.

Fig. S8 presents the geographical distribution of air–soil gas exchange flux of PAHs in the study area. Regions with higher exchange fluxes were mainly distributed in Tianjin, Baoding and Tangshan areas. Distribution pattern of air–soil gas exchange was different between summer and winter, but similar between spring and fall. Generally there was more air–soil gas exchange flux of PAHs in urban than remote and rural areas, more air to soil

deposition in urban areas, and more evaporation from soil to air in remote areas. Furthermore, in summer, the air–soil gas exchange flux of PAHs (except for BaA) in remote area was significantly lower compared to other rural village and urban areas ( $p < 0.05$ ) (Fig. 4), which is consistent with the lower  $f_f$  values in remote areas. In winter, the air–soil gas exchange flux in remote areas was also significantly lower relative to other areas ( $p < 0.05$ ) (Fig. 4). There was no significant difference of air–soil gas exchange flux between north rural village and north urban areas and between south rural village and south urban areas ( $p > 0.05$ ).

The spatial distribution of atmospheric PAH concentrations, meteorological conditions (temperature, humidity, and wind speed), vegetation cover, soil properties (total organic carbon (TOC) concentration, temperature, and humidity), and PAH emission sources, are all likely to impact the geographic distribution pattern of the air–soil gas exchange of PAHs (Cousins et al., 1999; Hippelein and McLachlan, 1998, 2000). Table S8 shows the correlation coefficients between soil TOC concentration and air–soil gas exchange flux of individual PAHs, and between the PAH emission density and the air–soil gas exchange flux of the individual PAHs. Figs. S9 and S10 show the scatter plots of the air–soil gas exchange flux of total PAH with TOC and emission density, respectively. No strong correlations were found between soil TOC concentration and the air–soil gas exchange flux for total PAH in any season (Fig. S9), and only a significantly positive correlation existed between the gas exchange flux of FLO and TOC concentration in the spring, summer and fall ( $p < 0.05$ ) (Table S6). However, there was a significant positive correlation between PAH emission density and the deposition flux of total PAHs from air to soil in winter ( $p < 0.01$ ) and approximately 57% of the total spatial variation of the exchange flux was explained by PAH emissions in winter (Fig. S10). A positive correlation was also found between the PAH emission density and the evaporation flux of total PAHs from soil to air in summer ( $p < 0.01$ ), but only 17% of the total spatial variation of the exchange flux was explained by PAH emissions in summer (Fig. S10). In addition, PAH emission was not an evident influence to air–soil gas exchange of total PAHs in spring and fall, but it was significantly correlated with evaporation flux of ACY and ACE from soil to air in spring (Table S8). In winter, there were more PAH emissions from residential heating, and the less efficient photochemical degradation of PAHs in air and lower mixing heights favor the accumulation of PAHs in the atmosphere, which resulted in more gaseous PAH deposition to soil from air. Low temperatures in winter also resulted in less evaporation of gaseous PAHs from soil to air. In summer, the air–soil gas exchange flux of PAHs can be influenced by rainfalls. High temperatures in summer are also in favor of evaporation of gaseous PAHs from soil to air. In summary, it appears that seasonality of the air–soil gas exchange fluxes of PAHs was governed by emission, meteorological conditions and soil TOC. It should be noted that the sampling heights varied among the sites and this difference may affect the PAH concentrations in the air leading to uncertainty to the results of air–soil gas exchange. It is recommended that more studies should be performed to address this effect quantitatively.

#### 4. Conclusion

A median total PAH (gaseous and particulate phase) concentration of  $349 \text{ ng/m}^3$  was measured at different sites in remote, rural village and urban areas of Beijing–Tianjin region from 2007 to 2008 ( $222 \text{ ng/m}^3$  for gaseous PAHs and  $114 \text{ ng/m}^3$  for particulate phase PAHs). Higher PAH concentrations were measured in winter compared to other seasons. PAH concentrations measured at the rural villages and urban sites in the northern mountain region were significantly lower than those measured at sites in the southern plain for all seasons. However, there was no significant difference in PAH concentrations between the rural villages and urban sites in the northern and southern areas. This urban–rural distribution pattern was related to the location of PAH emission sources and the population



density distribution. The PAH emission sources alone explain 56%–77% of the spatial variation in ambient air PAH concentrations. In summer, more gaseous PAHs evaporated from soil to air because of higher temperatures and increased rainfall. However, in winter, more gaseous PAHs deposited from air to soil due to higher PAH emissions and lower temperatures. The soil TOC concentration had no significant influence on air–soil gas exchange of PAHs.

## Supplementary Material

Refer to Web version on PubMed Central for supplementary material.

## Acknowledgments

This study is supported by National Basic Research Program (2007CB407301), National Science Foundation of China (grant 140710019001 and 40730737) and China Scholarship Council (to Wentao Wang). The project described was also supported by Award Number P42 ES016465 and P30ES00210 from the National Institute of Environmental Health Sciences. The content is solely the responsibility of the authors and does not necessarily represent the official views of the National Institute of Environmental Health Sciences or the National Institutes of Health.

## Appendix A. Supplementary data

Supplementary data to this article can be found online at doi:10.1016/j.scitotenv.2011.04.021.

## References

- Backea C, Cousins IT, Larsson P. PCB in soils and estimated soil–air exchange fluxes of selected PCB congeners in the South of Sweden. *Environ Pollut.* 2004; 128:59–72. [PubMed: 14667720]
- Bidleman TF, Leone A. Soil–air exchange of organochlorine pesticides in the southern United States. *Environ Pollut.* 2004; 128:49–57. [PubMed: 14667719]
- Bozlaker A, Odabasi M, Muezzinoglu A. Dry deposition and soil–air gas exchange of polychlorinated biphenyls (PCBs) in an industrial area. *Environ Pollut.* 2008a; 156:784–93. [PubMed: 18640753]
- Bozlaker A, Muezzinoglu A, Odabasi M. Atmospheric concentrations, dry deposition and air–soil exchange of polycyclic aromatic hydrocarbons (PAHs) in an industrial region in Turkey. *J Hazard Mater.* 2008b; 153:1093–102. [PubMed: 17977652]
- Bozlaker A, Muezzinoglu A, Odabasi M. Processes affecting the movement of organochlorine pesticides (OCPs) between soil and air in an industrial site in Turkey. *Chemosphere.* 2009; 77:1168–76. [PubMed: 19836050]
- Cetin B, Odabasi M. Particle-phase dry deposition and air–soil gas-exchange of polybrominated diphenyl ethers (PBDEs) in Izmir, Turkey. *Environ Sci Technol.* 2007; 41:4986–92. [PubMed: 17711213]
- Cousins IT, Jones KC. Air-soil exchange of semi-volatile organic compounds (SOCs) in the UK. *Environ Pollut.* 1998; 102:105–18.
- Cousins IT, Beck AJ, Jones KC. A review of the process involved in the exchange of semi-volatile organic compounds (SVOC) across the air-soil interface. *Sci Total Environ.* 1999; 228:5–24.
- Gioia R, Sweetman AJ, Jones KC. Coupling passive air sampling with emission estimates and chemical fate modeling for persistent organic pollutants (POPs): a feasibility study for Northern Europe. *Environ Sci Technol.* 2007; 41:2165–71. [PubMed: 17438758]
- Hafner WD, Carlson DL, Hites RA. Influence of local human population on atmospheric polycyclic aromatic hydrocarbon concentrations. *Environ Sci Technol.* 2005; 39:7374–9. [PubMed: 16245804]
- Harner T, Mackay D, Jones KC. Model of the long-term exchange of PCB between soil and the atmosphere in the southern UK. *Environ Sci Technol.* 1995; 29:1200–9. [PubMed: 22192012]

- Harner T, Bidleman TF, Jantunen LMM, Mackay D. Soil–air exchange model of persistent pesticides in the United States Cotton Belt. *Environ Toxicol Chem.* 2001; 20:1612–21. [PubMed: 11434306]
- Hippelein M, McLachlan MS. Soil/air partitioning of semivolatile organic compounds. 1. Method development and influence of physical-chemical properties. *Environ Sci Technol.* 1998; 32:310–6.
- Hippelein M, McLachlan MS. Soil/air partitioning of semivolatile organic compounds. 2. Influence of temperature and relative humidity. *Environ Sci Technol.* 2000; 34:3521–6.
- Klánová J, Kohoutek J, Hamplová L, Urbanová P, Holoubek I. Passive air sampler as a tool for long-term air pollution monitoring: part 1. Performance assessment for seasonal and spatial variations. *Environ Pollut.* 2006; 144:393–405. [PubMed: 16549225]
- Kobličková M, Růžičková P, Šupr P, Komprda J, Holoubek I, Klánová J. Soil burdens of persistent organic pollutants: their levels, fate, and risks. Part IV. Quantification of volatilization fluxes of organochlorine pesticides and polychlorinated biphenyls from contaminated soil surfaces. *Environ Sci Technol.* 2009; 43:3588–95. [PubMed: 19544859]
- Kurt-Karakus PB, Bidleman TF, Staebler RM, Jones KC. Measurement of DDT Fluxes from a historically treated agricultural soil in Canada. *Environ Sci Technol.* 2006; 40:4578–85. [PubMed: 16913109]
- Lang C, Tao S, Wang XJ, Zhang G, Li J, Fu JM. Seasonal variation of polycyclic aromatic hydrocarbons (PAHs) in Pearl River Delta region, China. *Atmos Environ.* 2007; 41:8370–9.
- Li YF, Harner T, Liu LY, Zhang Z, Ren NQ, Jia HL, et al. Polychlorinated biphenyls in global air and surface soils: distributions, air–soil exchange, and fractionation effect. *Environ Sci Technol.* 2010; 44:2784–90. [PubMed: 20384373]
- Liu SZ, Tao S, Liu WX, Liu YN, Dou H, Zhao JY, et al. Atmospheric polycyclic aromatic hydrocarbons in North China: a wintertime study. *Environ Sci Technol.* 2007; 41:8256–61. [PubMed: 18200848]
- Liu SZ, Tao S, Liu WX, Dou H, Liu YN, Zhao JY, et al. Seasonal and spatial occurrence and distribution of atmospheric polycyclic aromatic hydrocarbons in rural and urban areas of the North Chinese plain. *Environ Pollut.* 2008; 156:651–6. [PubMed: 18674851]
- Mackay D. Finding fugacity feasible. *Environ Sci Technol.* 1979; 13:1218–23.
- Mackay, D. Multimedia environmental models: the fugacity approach. Boca Raton FL: Lewis; 1991.
- Mackay D, Paterson S. Evaluating the multimedia fate of organic-chemicals – a level-III fugacity model. *Environ Sci Technol.* 1991; 25:427–36.
- Meijer SN, Shoeib M, Jantunen LMM, Jones KC, Harner T. Air–soil exchange of organochlorine pesticides in agricultural soils: 1. Field measurements using a novel in situ sampling device. *Environ Sci Technol.* 2003a; 37:1292–9.
- Meijer SN, Shoeib M, Jones KC, Harner T. Air–soil exchange of organochlorine pesticides in agricultural soils. 2. Laboratory measurements of the soil–air partition coefficient. *Environ Sci Technol.* 2003b; 37:1300–5.
- Nisbet C, LaGoy P. Toxic equivalency factors (TEFs) for polycyclic aromatic hydrocarbons (PAHs). *Regul Toxicol Pharmacol.* 1992; 16:290–300. [PubMed: 1293646]
- Okuda T, Naoi D, Tenmoku M, Tanaka S, He KB, Ma YL, et al. Polycyclic aromatic hydrocarbons (PAHs) in the aerosol in Beijing, China, measured by aminopropylsilane chemically-bonded stationary-phase column chromatography and HPLC/fluorescence detection. *Chemosphere.* 2006; 35:427–35. [PubMed: 16524620]
- Růžičková P, Klánová J, Šupr P, Lammel G, Holoubek I. An assessment of air–soil exchange of polychlorinated biphenyls and organochlorine pesticides across central and southern Europe. *Environ Sci Technol.* 2008; 42:179–85. [PubMed: 18350894]
- Sun P, Blanchard P, Brice KA, Hites RA. Trends in polycyclic aromatic hydrocarbon concentrations in the Great Lakes atmosphere. *Environ Sci Technol.* 2006; 40:6221–7. [PubMed: 17120545]
- Tao S, Liu WX, Li Y, Yang Y, Zuo Q, Li BG, et al. Organochlorine pesticides contaminated surface soil as reemission source in the Haihe Plain, China. *Environ Sci Technol.* 2008; 42:8395–400. [PubMed: 19068823]
- Tao S, Cao J, Wang WT, Zhao JY, Wang W, Wang ZH, et al. A passive sampler with improved performance for collecting gaseous and particulate phase polycyclic aromatic hydrocarbons in air. *Environ Sci Technol.* 2009; 43:4124–9. [PubMed: 19569340]

- Wang DG, Yang M, Jia HL, Zhou L, Li YF. Seasonal variation of polycyclic aromatic hydrocarbons in soil and air of Dalian areas, China: an assessment of soil–air exchange. *J Environ Monit.* 2008a; 10:1076–83. [PubMed: 18728901]
- Wang XF, Cheng HX, Xu XB, Zhuang GM, Zhao CD. A wintertime study of polycyclic aromatic hydrocarbons in PM<sub>2.5</sub> and PM<sub>2.5–10</sub> in Beijing: assessment of energy structure conversion. *J Hazard Mater.* 2008b; 157:47–56. [PubMed: 18342441]
- Wang WT, Simonich SM, Xue M, Zhao JY, Zhang N, Wang R, et al. Concentrations, sources and spatial distribution of polycyclic aromatic hydrocarbons in soils from Beijing, Tianjin and surrounding areas, North China. *Environ Pollut.* 2010; 158:1245–51. [PubMed: 20199833]
- Wong F, Alegria HA, Bidleman TF. Organochlorine pesticides in soils of Mexico and the potential for soil–air exchange. *Environ Pollut.* 2010; 158:749–55. [PubMed: 19910095]
- Wu SP, Tao S, Liu WX. Particle size distributions of polycyclic aromatic hydrocarbons in rural and urban atmosphere of Tianjin, China. *Chemosphere.* 2006; 62:357–67. [PubMed: 15982711]
- Wu SP, Tao S, Zhang ZH, Lan T, Zuo Q. Characterization of TSP-bound n-alkanes and polycyclic aromatic hydrocarbons at rural and urban sites of Tianjin, China. *Environ Pollut.* 2007; 147:203–10. [PubMed: 17029681]
- Zhang YX, Tao S. Seasonal variation of polycyclic aromatic hydrocarbons (PAHs) emissions in China. *Environ Pollut.* 2008; 156:657–63. [PubMed: 18649978]
- Zhang YX, Tao S. Global atmospheric emission inventory of polycyclic aromatic hydrocarbons (PAHs) for 2004. *Atmos Environ.* 2009; 43:812–9.
- Zhang YX, Tao S, Cao J, Coveney RM. Emission of polycyclic aromatic hydrocarbons in China by county. *Environ Sci Technol.* 2007; 41:683–7. [PubMed: 17328170]
- Zhang YX, Tao S, Shen HZ, Ma JM. Inhalation exposure to ambient polycyclic aromatic hydrocarbons and lung cancer risk of Chinese population. *Proc Natl Acad Sci USA.* 2009; 106:21063–7. [PubMed: 19995969]
- Zhou JB, Wang TG, Huang YB, Mao T, Zhong NN. Size distribution of polycyclic aromatic hydrocarbons in urban and suburban sites of Beijing, China. *Chemosphere.* 2005; 61:792–9. [PubMed: 15927233]

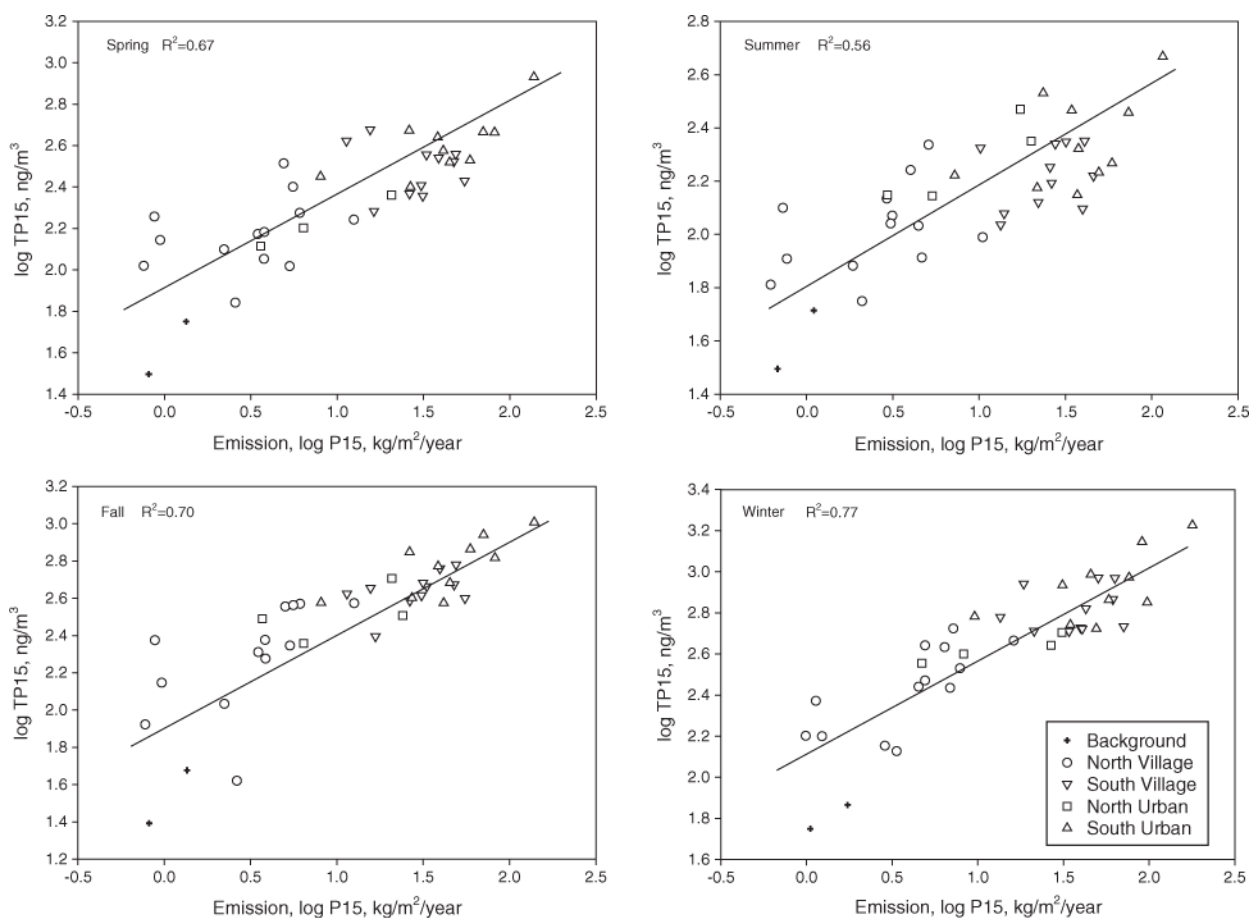


**Fig. 1.** Scatter plots of ambient air PAH concentrations and PAH emission density in spring, summer, fall and winter. TP15 on the Y-axis represents the total PAH concentration (sum of gas-phase and particulate-phase concentrations of the 15 PAHs). P15 on the X-axis represents the emission density of the 15 PAHs.

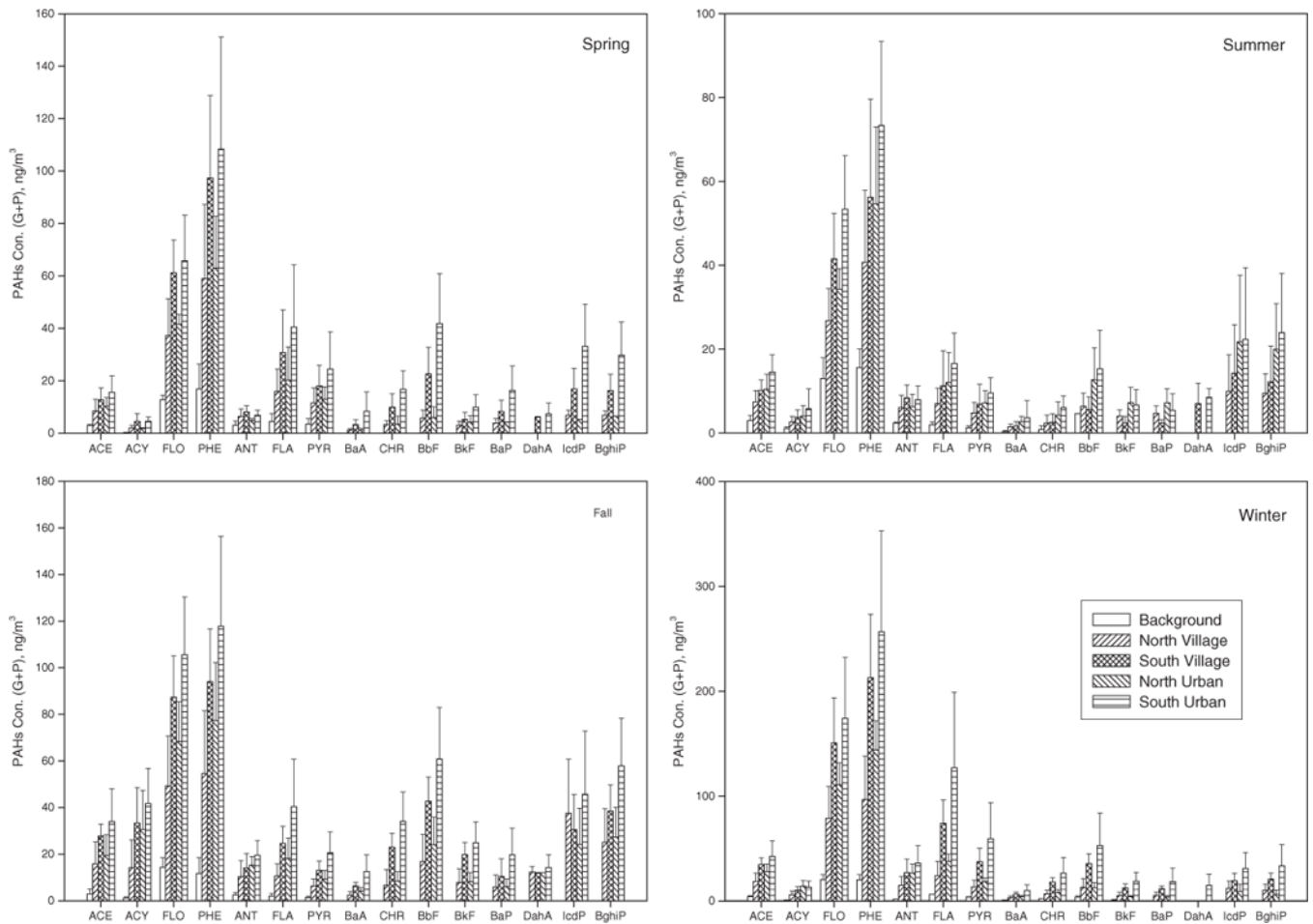


**Fig. 2.** The individual PAH concentrations (gas-phase + particulate-phase PAHs) in background, northern rural village, southern rural village, northern urban and southern urban areas in spring, summer, fall and winter.



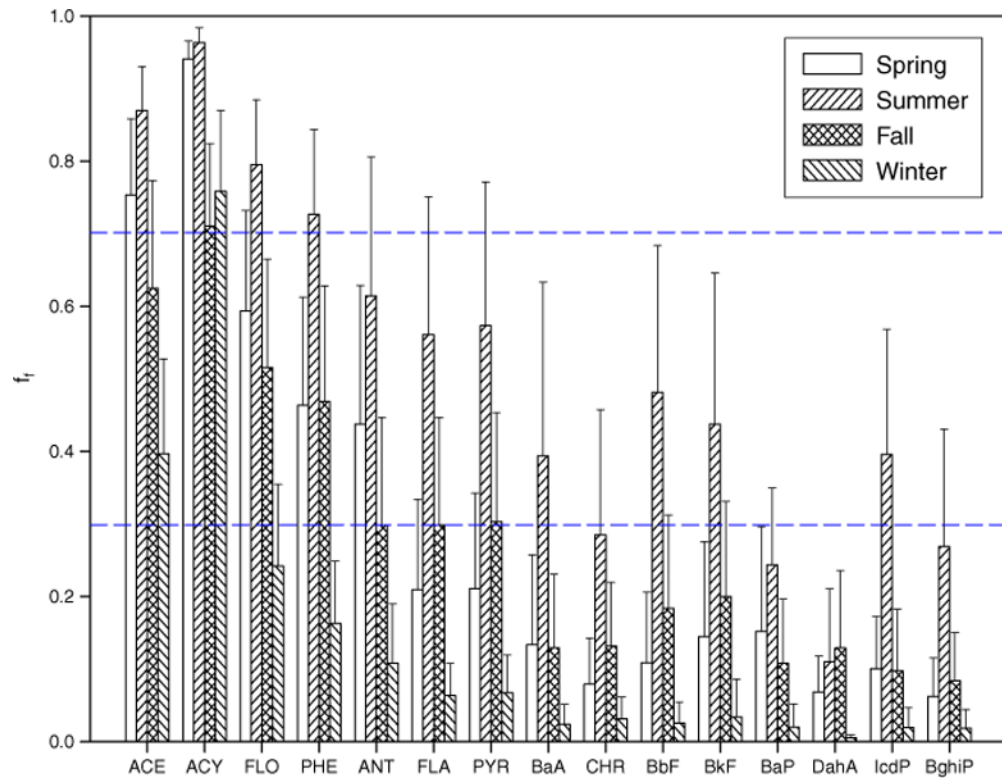


**Fig. 3.** Fugacity fraction ( $f_i$ ) values of individual PAHs for spring, summer, fall and winter (error bar represents standard deviation of  $f_i$  values).

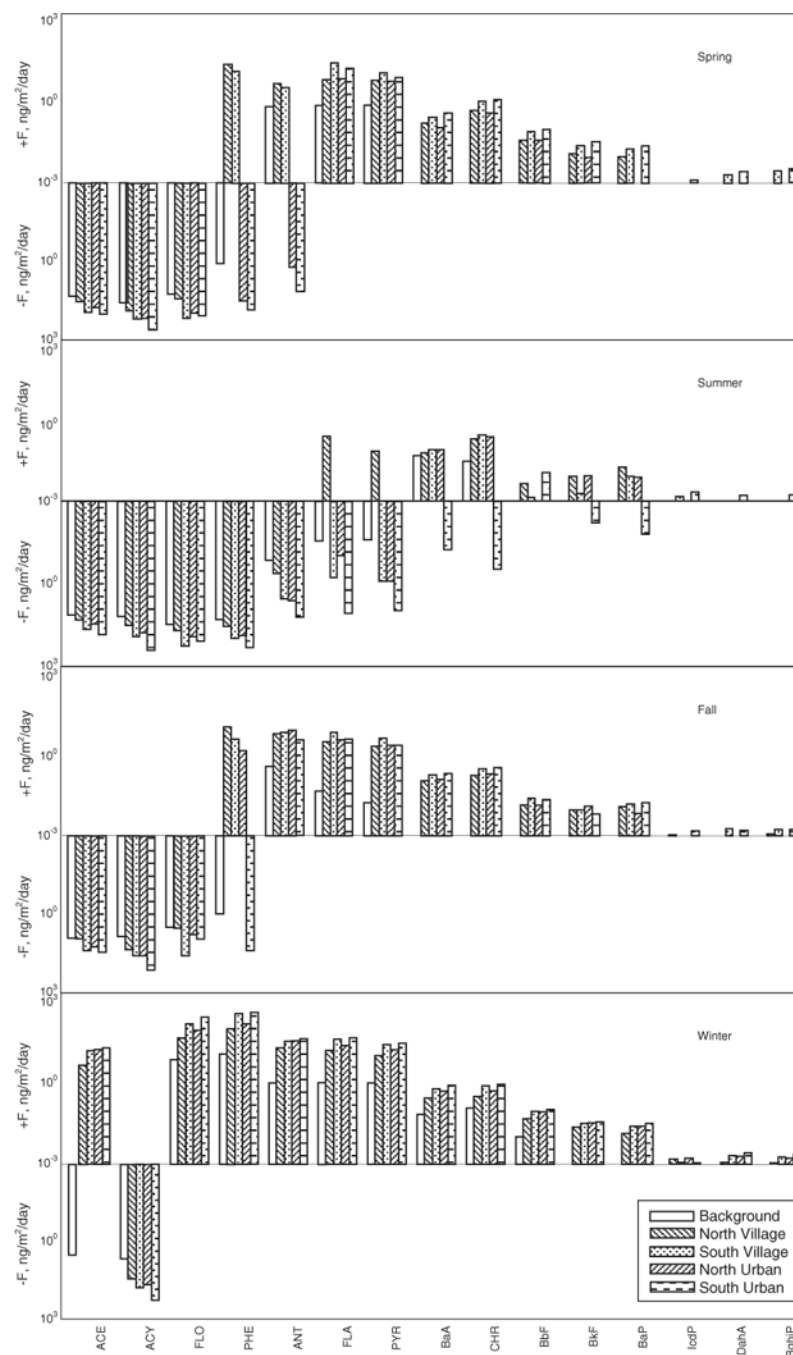


**Fig. 4.** Air–soil exchange fluxes of gaseous PAHs in background, northern village, southern village, northern urban and southern urban areas for four seasons. Negative flux values indicate the air–soil exchange of PAHs is from soil to air and positive flux values indicate the air–soil exchange of PAHs is from air to soil.